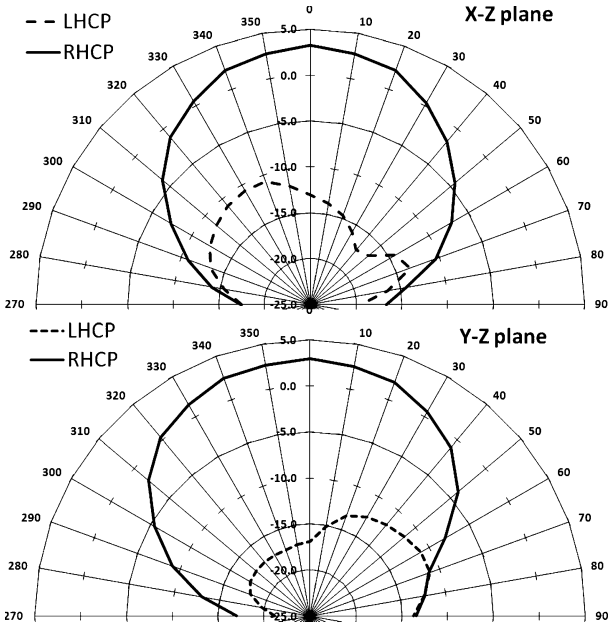

Fig. 8. The measured radiation patterns at 2.45 GHz.

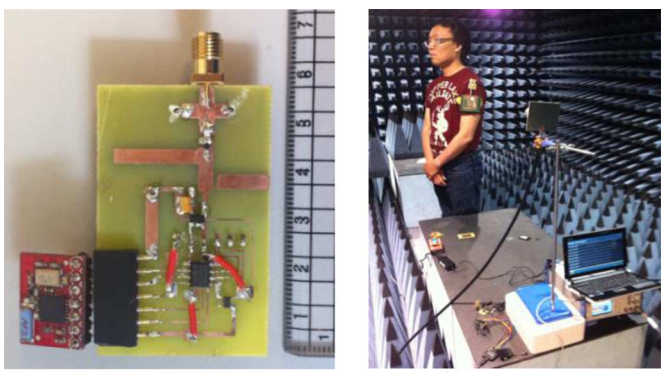

(a) (b)

Fig. 9. (a) The transponder. (b) Testing on a human arm inside the chamber.

single-fed to produce circular polarization. The textile antenna is bent on a human arm with the wirelessly-powered sensor system proved to be operational over a 1.7-meters range with under 0.05 W power transmitted from a base station. This demonstrates that a robust and ultra low-power battery-less μC sensor platform can be implemented and integrated into clothes for other sensing applications in the future.

REFERENCES

[1] E. K. Kaivanto, M. Berg, E. Salonen, and P. de Maagt, "Wearable circularly polarized antenna for personal satellite communication and navigation," *IEEE Trans. Antennas Propag.*, vol. 59, no. 12, pp. 4490–4496, Dec. 2011.

[2] L. Vallozzi, P. Van Torre, C. Hertleer, and H. Rogier, "A textile antenna for off-body communication integrated into protective clothing for firefighters," *IEEE Trans Antennas Propag.*, vol. 57, no. 4, pp. 919–925, Apr. 2009.

[3] D. Masotti, A. Costanzo, and S. Adami, "Design and realization of a wearable multi-frequency RF energy harvesting system," in *Proc. 5th Eur. Conf. Antennas Propag.*, Apr. 11–15, 2011, pp. 517–520.

[4] E. Kaivanto, J. Lilja, M. Berg, E. Salonen, and P. Salonen, "Circularly polarized textile antenna for personal satellite communication," in *Proc. 4th Eur. Conf. Antennas Propag.*, Apr. 12–16, 2010, pp. 1–4.

[5] M. Klemm, I. Locher, and G. Troster, "A novel circularly polarized textile antenna for wearable applications," in *Proc. 7th Eur. Conf. Wireless Tech.*, Oct. 12, 2004, pp. 285–288.

[6] J.-Y. Sze and W.-H. Chen, "Axial-ratio-bandwidth enhancement of a microstrip-line-fed circularly polarized annular-ring slot antenna," *IEEE Trans. Antennas Propag.*, vol. 59, no. 7, pp. 2450–2456, Jul. 2011.

[7] J.-Y. Sze, C.-I. G. Hsu, Z.-W. Chen, and C.-C. Chang, "Broadband CPW-Fed circularly polarized square slot antenna with lightening-shaped feedline and inverted-L grounded strips," *IEEE Trans. Antennas Propag.*, vol. 58, no. 3, pp. 973–977, Mar. 2010.

[8] K. W. Lui, O. H. Murphy, and C. Toumazou, "32 μW wirelessly-powered sensor platform with a 2-m range," *IEEE Sensors J.*, vol. 12, no. 6, pp. 1919–1924, Jun. 2012.

[9] "EMI Flectron Metallized Fabrics Specification Sheet," Lairtech Technologies, 1998.

[10] C. C. Chou, K. H. Lin, and H. L. Su, "Broadband circularly polarised crosspatch-loaded square slot antenna," *Electron. Lett.*, vol. 43, no. 9, pp. 485–486, Apr. 26, 2007.

[11] R. Fossi, C. Petrucci, and D. Andreuccetti, Calculation of the Dielectric Properties of Body Tissues in the Frequency Range 10 Hz–100 GHz [Online]. Available: http://niremf.ifac.cnr.it/tissprop/ 1997

[12] M. Klemm and G. Troester, "Textile UWB antennas for wireless body area networks," *IEEE Trans. Antenna Propag.*, vol. 54, no. 11, pp. 3192–3197, Nov. 2006.

[13] H. Giddens, D. L. Paul, G. S. Hilton, and J. P. McGeehan, "Influence of body proximity on the efficiency of a wearable textile patch antenna," in *Proc. 6th Eur. Conf. Antennas Propag.*, Mar. 26–30, 2012, pp. 1353–1357.

A Dual Band Leaky Wave Antenna on a CRLH Substrate Integrated Waveguide

Jan Machac, Milan Polivka, and Kirill Zemlyakov

***Abstract*—This communication presents the results of an investigation of a new version of a leaky wave antenna designed on a CRLH substrate integrated waveguide. The antenna operates in two frequency bands and its main beam can be steered from backward to forward direction by changing the frequency. The antenna structure is planar and can be fabricated by a standard PCB technology, so it is suitable for mass production. An efficient method for determining the complex dispersion characteristic of periodic 1D structure is proposed.**

***Index Terms*—Composite right/left-handed transmission line, leaky wave antenna, substrate integrated waveguide.**

I. INTRODUCTION

Low profile planar antennas can be integrated with other circuits and can be easily fabricated. They are therefore suitable for cheap mass production. They have been of great interest to researchers and designers

Manuscript received November 01, 2012; revised February 10, 2013; accepted March 16, 2013. Date of publication April 02, 2013; date of current version July 01, 2013. This work was supported by the Grant Agency of the Czech Republic under the project 13-09086S, and by the Czech Technical University in Prague under the project OHK3-011/13.

J. Machac and M. Polivka are with the Department of Electromagnetic Field, Technical University in Prague, 16627 Praha 6, Czech Republic (e-mail: polivka@fel.cvut.cz; machac@fel.cvut.cz).

K. Zemlyakov is with St. Petersburg Electrotechnical University, 197376 St. Petersburg, Russia (e-mail: kirill.zemlyakov@gmail.com).

Color versions of one or more of the figures in this communication are available online at http://ieeexplore.ieee.org.

Digital Object Identifier 10.1109/TAP.2013.2256097

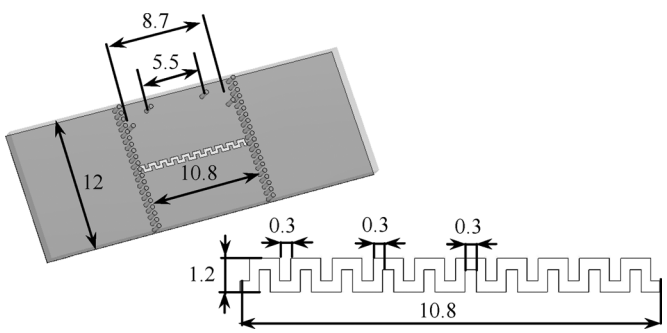

Fig. 1. Layout of the meander slot and the SIW unit cell set up.

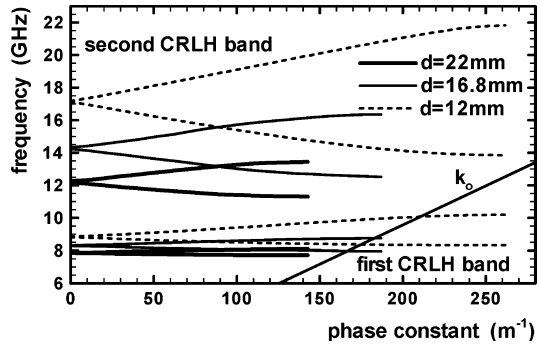

Fig. 2. Dispersion characteristics of the SIW LWA for different cell lengths. These three antennas also differ in SIW width.

for more than thirty years. A substrate integrated waveguide (SIW) is a possible version of a low profile planar transmission line that can be simply designed and fabricated [1]. The SIW LWA concept was proposed in [2]. This antenna radiates energy through the SIW side wall with sparsely located shortening vias. The concept of an LWA based on radiation through the wide slot in the SIW top wall due to a leaky wave of the first order was proposed in [3]. The SIW designed as a balanced right/left-handed (CRLH) transmission line was used as an LWA able to steer the radiation pattern main beam by changing the frequency from nearly backward direction to forward direction [4], [5].

A line offering CRLH behavior in two frequency bands was proposed in [6], where the condition for this feature was derived.

A new dual band SIW LWA based on the CRLH line working in two frequency bands proposed in this communication was designed and fabricated. The idea and the design are inspired by the antenna structure originally presented in [7]. The antenna radiates one main beam that can be steered from the backward direction to the forward direction by changing the frequency in both frequency bands. Radiation occurs through meander slots etched in the top metallization wall. The measured antenna characteristics are in good agreement with those predicted by the simulation.

The antenna complex dispersion characteristics are studied in detail, and an efficient method for determining them is proposed.

II. Design of a Dual Band CRLH SIW Unit Cell

The idea of the antenna design is based on conclusions of [6] concerning dual band/quad band operation of the CRLH transmission line. The equivalent circuit of such a line is composed of series and parallel resonant LC circuits compositions in both the through and shunt branches that is respected by the proposed antenna unit cell structure shown in Fig. 1. The series elements are represented mainly by the meander slots that enable the antenna to radiate, see the detail in Fig. 1. The parallel elements are represented by four conducting vias. All these elements are however mutually coupled, and the equivalent circuit of the cell (not shown in this communication) derived from its dispersion characteristic fully corresponds to the equivalent circuit presented in [6].

An analysis of the SIW antenna structure was performed by the CST Microwave Studio (CST MWS) using solid PEC walls terminating the SIW from the sides in order to simplify the computation process. A Rogers RO4003C substrate 1.524 mm in thickness with relative permittivity 3.38 ± 0.05 and loss factor 0.002 was used. The presented structure was designed with the aim to reduce the reflection losses and at the same time to improve the radiation pattern shape, i.e., to reduce the spurious radiation that occurred in the original structure [7].

The spurious radiation is due to the Bragg reflection that occurs if the condition

$$\beta d = \pi \tag{1}$$

is fulfilled. β is phase constant, d is the cell length. This happens at the edges of the dispersion characteristics branches.

Fig. 2 shows the dispersion characteristics of three antennas differing particularly by the unit cell length. It follows from this plot that the cell length determines mainly the central frequency of the upper band, whereas the central frequency of the first band is mainly determined by the SIW width. The design of the three antennas was performed by the CST MWS, with the aim to close the bands between the LH and RH bands. However, there are finally some gaps left. For the presented structure with the cell 12 mm in length, these are 25 and 85 MHz. Fig. 2 shows the dependence of the free space propagation constant k_{o} on frequency, which represents the boundary between the radiating area, where $\beta < k_{\mathrm{o}}$, and the non-radiating area. If (1) is fulfilled, spurious radiation occurs. This can be removed by shifting this point into a non-radiating area, or at least to the close proximity of it. The drawback is of course that the steering beam span is reduced.

The radiation pattern was predicted by substituting the antenna by an array of radiating elements representing the meander slots. The cell length, i.e., the element distance of this array that ensures the structure without the spurious radiation reported in [7], was found to be 11 mm. Finally the antenna structure was designed having the cell 12 mm in length. This is a compromise between a length of 11 mm, suggested by the approximate analysis, and the design aimed at closing the gaps between the LH and RH bands. The final dimensions of the unit cell are shown in Fig. 1.

III. Dispersion Characteristic, Equivalent Circuit

The dispersion characteristics; see Fig. 2 show clearly the antenna dual band operation. The complex propagation constant of an infinitely long periodic 1D structure $\gamma = \alpha + j\beta$, where α is attenuation constant and β is phase constant was calculated as [8],

$$\cosh(\gamma d) = \frac{A + D}{2} \tag{2}$$

where A, D are elements of the ABCD transmission matrix $\mathbf{A}$.

The periodic transmission line is composed of a chain of elementary cells that are tightly coupled, and additionally the behavior of the first cell and the last cell is modified by the presence of a source used to calculate or to measure the transmission matrix. The behavior of an "inner" cell that includes the coupling with all neighbor cells can be

obtained from calculated or measured transmission matrix $\mathbf{A}_c$ of the chain containing N cells. The ABCD matrix of one cell is

$$\mathbf{A} = \sqrt[N]{\mathbf{A}_c}. \tag{3}$$

The N-th root of a matrix is calculated as

$$\mathbf{A} = \exp\left[\frac{1}{N}\ln\left(\mathbf{A}_c\right)\right]. \tag{4}$$

Only the basic branch of the logarithm function is taken into account, the ambiguity is removed by calculating the dispersion characteristic by (2) based on a rough knowledge of the frequency centers of the two antenna frequency bands. This distinguishes our method from those proposed in [9]. A procedure equivalent to (2)–(4) is presented in [8]. It is applied not to determine the dispersion characteristic but the parameters of the cell equivalent circuit.

The procedure represented by (2)–(4) was applied to the SIW LWA described in the previous paragraph. The convergence is relatively fast, apart from the values in the stop bands below 8.4 GHz and between 10.2 and 13.8 GHz. So finally $N = 9$ is a sufficient number of cells. The analysis was done at CST MWS. The provided data describes the analyzed periodic structure very rigorously.

The dispersion characteristics were alternatively determined by the CST MWS eigenmode solver, as those in Fig. 2. This solver takes into account only lossless resonators, so only the real resonant frequency can be determined and, using this way, only the phase constant can be calculated. The radiation cannot be accounted for. The analyzed unit cell must be fully enclosed. So it was terminated by periodic boundaries in longitudinal direction, PEC and PMC walls from bottom and top and PMC walls from the sides. PMC walls correspond better to the field of the radiated wave than PEC walls. The values are plotted in Fig. 3, marked as "eigen". The agreement with data determined by (2)–(4) is excellent, with the exception of the LH1 band. The phase constant β determined by the argument of S_{21} of one cell as

$$\beta = -\arg\left(S_{21}\right)/d \tag{5}$$

fits well the data shown in Fig. 3 around the frequency points where $\beta = 0$. This substitution is of course not valid near the Bragg reflection condition (1). The real part of the complex propagation constant representing the attenuation due to radiation and losses could also be evaluated from the cell radiation losses as

$$\alpha = -\ln\sqrt{|S_{11}|^2 + |S_{21}|^2}\Big/ d \tag{6}$$

using the scattering parameters calculated by CST MWS. The data obtained by the procedure described by (2)–(4) takes into account all losses in the dielectric, in metal, and the radiation. The line denoted as atten. "N = 9" in Fig. 3(b) therefore shows the correct values of the attenuation constant. The attenuation constant calculated by (6) represents the power lost in the structure combined with the power reflected from the structure, so it does not really correspond to the periodic line. Nevertheless it serves as some estimate of the attenuation constant within the LH and RH bands; see the line denoted "Eq. (6)" in Fig. 3.

IV. Antenna Design and Experiment

Matching circuits were designed for antennas consisting of 15 cells and 25 cells correspondingly, with unit cell length equal to 12 mm. A quarter-wavelength transformer was used to transform the real part of

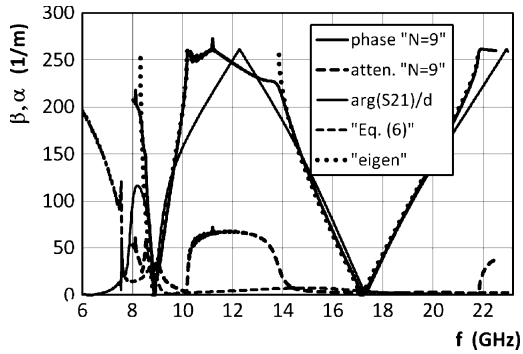

Fig. 3. Phase and attenuation constants of the LWA with $d = 12$ mm. Particular lines are described in the text.

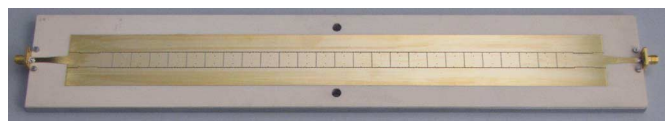

Fig. 4. The fabricated SIW leaky wave antenna with 25 cells.

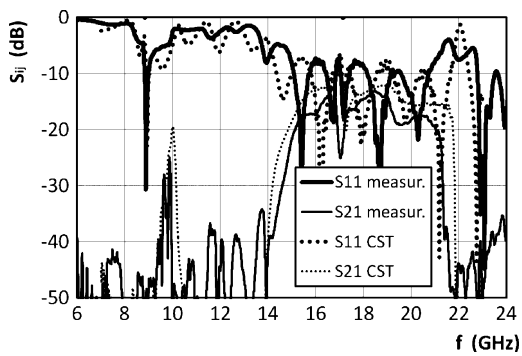

Fig. 5. Calculated and measured scattering parameters of the antenna with 25 cells.

Z_{in} to nearly the same value as the impedance of the empty SIW. The transformer was located at the point where $\mathrm{Im}(Z_{in})$ is almost equal to zero. The main advantage of this type of matching is that it matches the first band of the antenna, making coefficient S_{11} in the center of the first band better, but it simultaneously does not affect the second band of the antenna.

The SIW periodic antenna structure is connected to the input and output 50 Ω SMA connectors via tapered microstrip line transitions [1]. The designed antenna was fabricated by a planar printed circuit board technology in two specimens differing by the number of cells. The shorter antenna has 15 cells, the longer antenna has 25 cells. A photograph of the longer antenna is shown in Fig. 4.

The scattering parameters of the fabricated antennas were measured, and are compared in Fig. 5 with the parameters calculated by CST MWS. The simulated and measured data matches relatively well.

The radiation patterns of the longer antenna with 25 cells taken in the longitudinal plane normal to the antenna surface were calculated by CST MWS and also measured; see Fig. 6.

Angle θ Was measured from the backward direction and equals 90 deg at broadside. The patterns show the main advantage of an LWA based on the CRLH line, steering the direction of the main lobe from backward direction to forward direction by changing the frequency in the two frequency bands. The behavior of the shorter antenna is similar except that the beams are wider.

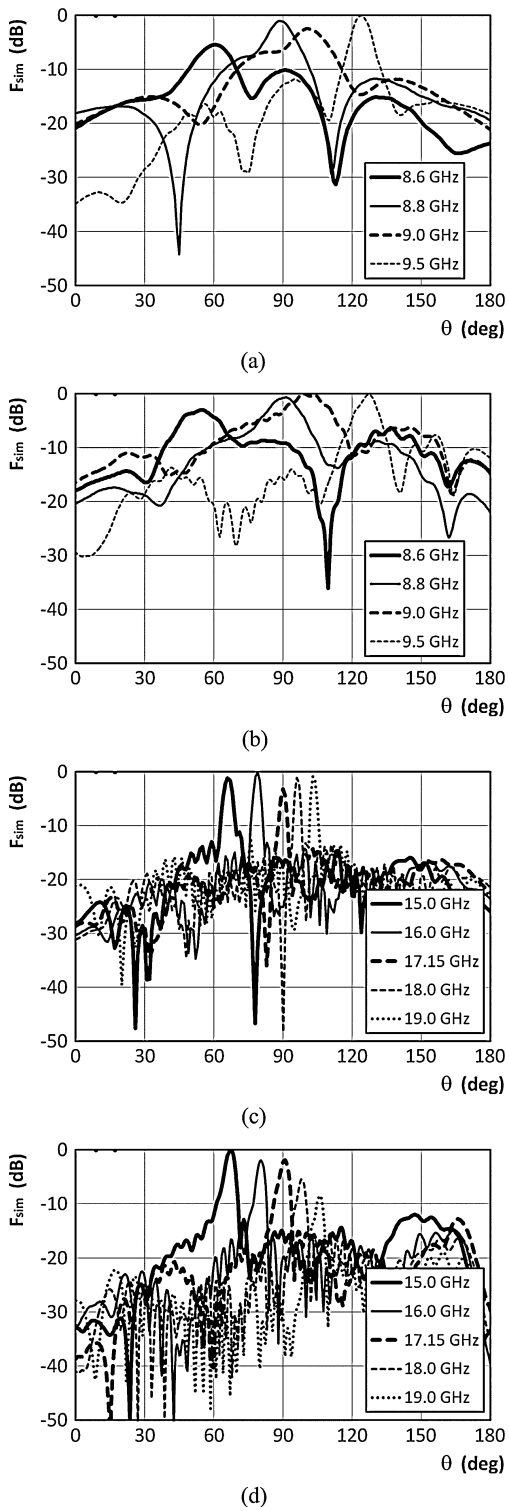

Fig. 6. Calculated and measured radiation patterns of the longer antenna for varying frequency in the first band (a), (b), and in the second band (c), (d), respectively.

The narrow main beam is present from about 8.6 up to 9.5 GHz in the lower CRLH band. The main lobe of the radiation pattern can be steered from 65 to 125 deg in this frequency band. Radiation patterns exhibit spurious side lobes around 150 deg that are only about 6 to 10 dB lower than the main lobes. These lobes are caused by spurious radiation of the SMA-microstrip transition, as characteristics calculated for the antenna model without these transitions are free of this spurious radiation.

The second CRLH band is wider than the first band. The narrow pencil beam, which is narrower than in the lower band, spans from about 15.0 up to 19.0 GHz. The beam steering is less sensitive here, and can be done in the span of 65 to 105 deg. The radiation patterns suffer from the existence of a side lobe, directed in elevation angles between 130 and 170 deg., which is about 6 to 12 dB smaller in the measured plots than the main beam. The decrease in antenna efficiency with increasing frequency may be due to residual radiation of the feeding cables used in the measurement setup but not included in the EM model.

The antenna gain, evaluated by the comparison method using DRH20 measurement double ridge horns, see [10], is 6.5 and 16.0 dBi at 8.8 and 17.15 GHz, respectively.

V. Conclusion

A dual band substrate integrated waveguide leaky wave antenna was designed, fabricated and measured. The balanced CRLH substrate integrated waveguide was used to give the possibility to scan the radiated beam from the forward direction to the backward direction by changing the frequency. The antenna radiates narrow beams in two frequency bands spanned from approx. 8.6 up to 9.5 GHz and from 15.0 up to 19.0 GHz. The exact scanning ability is 60 deg across the broadside direction in the lower band and about 40 deg across the broadside direction in the upper band. The complex dispersion characteristics were determined by a new efficient method proposed in this communication that can be considered as a unique source of data applicable to a wide class of radiating periodic structures. The analysis performed by CST Microwave Studio verifies the measured antenna characteristics well.

The designed antenna is aimed for integration into antenna arrays and into transmitting or receiving systems where beam scanning and double band operation are required at the same time. The standard PCB process is applied for fabricating this antenna, making cheap mass production possible.

References

[1] D. Deslandes and K. Wu, "Single-substrate integration technique of planar circuits and waveguide filters," *IEEE Trans. Microw. Theory Tech.*, vol. 51, no. 2, pp. 593–596, Feb. 2003.

[2] D. Deslandes and K. Wu, "Substrate integrated waveguide leaky-wave antenna: Concept and design considerations," presented at the Asia Pacific Microw. Conf., Suzhou, China, Dec. 2005.

[3] J. Machac, P. Lorenz, M. Saglam, C.-T. Bui, and W. Kraemer, "Substrate integrated waveguide leaky wave antenna radiating from a slot in the broad wall," presented at the IEEE MTT-S Int. Microw. Symp., May 2010, TU1A-2.

[4] Y. D. Dong and T. Itoh, "Composite right/left-handed substrate integrated waveguide and half mode substrate integrated waveguide leaky-wave structures," *IEEE Trans. Antennas Propag.*, vol. 59, no. 3, pp. 767–775, Mar. 2011.

[5] Y. Weitsch and T. F. Eibert, "Composite right-/left-handed interdigital leaky-wave antenna on a substrate integrated waveguide," presented at the 4th Eur. Conf. Antennas Propagation, Barcelona, Spain, Apr. 2010.

[6] G. V. Eleftheriades, "A generalized negative-refractive-index transmission-line (NRI-TL) metamaterial for dual-band and quad-band applications," *IEEE Microw. Wireless Compon. Lett.*, vol. 17, no. 6, pp. 415–417, Jun. 2007.

[7] J. Machac and M. Polivka, "A dual band SIW leaky wave antenna," presented at the IEEE MTT-S Int. Microwave Symp., Jun. 2012, WE4J-4.

[8] S. Otto, A. Rennings, K. Solbach, and C. Caloz, "Transition line modelling and asymptotic formulas for periodic leaky-wave antennas scanning through broadside," *IEEE Trans. Antennas Propag.*, vol. 59, no. 10, pp. 3695–3709, Oct. 2011.

[9] G. Valerio, S. Paulotto, P. Baccarelli, P. Burghignoli, and A. Galli, "Accurate Bloch analysis of 1-D periodic lines through the simulation of truncated structures," *IEEE Trans. Antennas Propag.*, vol. 59, no. 6, pp. 2188–2195, Jun. 2011.

[10] RFspin, s.r.o.. Prague, Czech Republic, Datasheet of Double Ridged Waveguide Horn—Model DRH20 [Online]. Available: http://www.rf-spin.cz/anteny/drh20.php 2013